

Coulomb-Gas Scaling Law for a Superconducting $\text{Bi}_{2+y}\text{Sr}_{2-x-y}\text{La}_x\text{CuO}_{6+\delta}$ Thin Films in Magnetic Fields

Y. Z. Zhang,^{1,2} R. Deltour,¹ and Z. X. Zhao²

¹*Université Libre de Bruxelles, Physique des Solides, B-1050, Brussels, Belgium*

²*National Laboratory for Superconductivity, Institute of Physics & Centre for Condensed Matter Physics, Chinese Academy of Sciences, P.O. Box 603, Beijing 100080, China*

(Received 3 September 1999; revised manuscript received 10 July 2000)

The electrical transport properties of epitaxial superconducting $\text{Bi}_{2+y}\text{Sr}_{2-x-y}\text{La}_x\text{CuO}_{6+\delta}$ thin films have been studied in magnetic fields. Using a modified Coulomb-gas scaling law, we can fit all the magnetic field dependent low resistance data with a universal scaling curve, which allows us to determine a relation between the activation energy of the thermally activated flux flow resistance and the characteristic temperature scaling parameters.

PACS numbers: 74.60.Ge, 74.25.Dw, 74.76.-w

High- T_c superconductors (HTSCs) consist of alternate stacking of superconducting (CuO_2) and non(or weakly-)superconducting layers [1–3]. The superconducting layers are coupled together through proximity and Josephson effects while thermal energy fluctuations and magnetic fields favor their decoupling. This competition leads to interlayer vortex coupling and decoupling, very similar to the vortex-antivortex pairs binding and unbinding described by the Kosterlitz-Thouless (KT) transition [4,5]. When a magnetic field is applied along the c axis (perpendicular to the CuO_2 layers) of a quasi-two-dimensional (2D) HTSC, the flux lines consist of pancake vortices [1–3] coupled together through their interlayer and intralayer interactions. Above a certain temperature the interactions can be substantially reduced, resulting in free 2D vortices in each CuO_2 layer. Minnhagen *et al.* suggested that Coulomb-gas (CG) scaling law could be applied to analyze these free 2D vortices [6–8] and we have extended their analysis to study these highly anisotropic HTSC superconductors in magnetic fields. In this article, we report the electrical transport measurements of epitaxial superconducting Bi-2201 thin films in magnetic fields up to 5.0 T. Using the modified CG scaling law for scaling the temperature and field dependences of the low resistance data $R(T, H)$ tails, we find that all the $R(T, H)$ curves fall onto a universal CG curve with the CG characteristic temperatures directly related to the magnetic field dependent activation energy.

$\text{Bi}_{2+y}\text{Sr}_{2-x-y}\text{La}_x\text{CuO}_{6+\delta}$ (Bi-2201) is a La doped HTSC and one of the members of BiSrCaCuO (BSCCO) superconductors. The ideal composition of the compound is $y = 0$. However, this compound is a solid solution and the actual range of y is still in debate [9,10]. Without La doping ($x = 0$), excess holes lead to a nonsuperconducting transition [11]. A little deviation of the atomic ratio, Bi:Sr, is required to obtain a superconducting phase ($T_c < 10$ K). However, deviations from a 1/1 ratio are very limited, Bi:Sr \in (1.05–1.11) [12], the substitution of La^{3+} for Sr^{2+} compensating the excess of holes in the CuO_2 layers [11,12]. The superconducting properties also

depend on the La content for which an optimal amount is approximately $x \approx 0.4$ ($T_c \rightarrow 40$ K) [13]. Bi-2201 has one of the simplest HTSC structures with one CuO_2 unilayer per half-unit cell (≈ 1.22 nm) and shows highly anisotropic properties (quasi-2D) with a very large anisotropic factor, $\gamma^2 = 3 \times 10^3 \sim 2 \times 10^5$ [14,15], providing a limiting case for the understanding of quasi-2D behavior in layered superconductors.

Compared to a single crystal, an epitaxial thin film offers a great facility to study the transport properties of a HTSC [16]. We have prepared high-quality, epitaxial Bi-2201 thin films on (100) SrTiO_3 and (100) LaAlO_3 substrates by magnetron sputtering [15]. Changing the atomic ratio of La for Sr in a series of Bi-2201 targets or adjusting the oxygen amount through different annealing processes, we have prepared underdoped, optimally doped, and overdoped samples, the highest transition temperature being 30 K for an optimally doped thin film. The structures and morphologies of the films were determined by x-ray diffraction, microscope transmission electron microscopy, atomic force microscopy, and scanning electron microscopy. The thin films are c -axis oriented and without secondary phases. A main difference between thin films and single crystals is that the films contain extended defects, such as 90° twins, and mismatches. These defects break the order parameters of the vortex lattice and enhance the vortex pinning in magnetic fields. In this case, the vortex glass and a second order glass transition can be expected in thin films.

According to the CG scaling expressions for $R(T, H)$ data [6], we make three assumptions. First, we assume that the $R(T, H)$ tail can be scaled by a universal function

$$\ln[R(T, H)/R_N] = \ln[R^*(X)/R_N], \quad (1)$$

with

$$X(T, H) = \frac{T[T_X(H) - T_{c0}(H)]}{T_{c0}(H)[T_X(H) - T]}, \quad \text{for } T < T_X, \quad (2)$$

where T_{c0} is analogous to T_{KT} for the KT transition, T_X is the mean field transition temperature, and X the scaling

variable in the CG scaling. Here, $X(T, H)$ is only magnetic field dependent through $T_{c0}(H)$ and $T_X(H)$. Second, we assume that the $R(T, H)$ tail can be scaled by the Halperin and Nelson relation $R(T, H) = R_N \exp\{-A/[X(T, H) - 1]^{1/2}\}$ [5], where A is a constant. This implies that the resistive tail data will fall onto the single curve

$$\ln[R^*(X)/R_N] = -A/(X - 1)^{1/2}. \quad (3)$$

Third, using the power law, $V \propto I^{\alpha+1}$, for I - V isotherms, we assume that $T_{c0}(H)$ is the characteristic temperature, at which $\alpha = \alpha(H) \rightarrow 2$, allowing all the $\ln[R(T, H)/R_N]$ curves to collapse onto a universal curve. This power law mimics the power law of the KT transition [6–8], $V \propto I^{\alpha+1}$ with $\alpha = 2$, and also the vortex glass scaling $V \sim I^{(z+1)/(d-1)}$ with $d = 2$ and $z = 2$ (or with $d = 3$ and $z = 5$) [1–3,17–21].

To test the modified CG scaling law, we applied this scaling analysis on several sample data [$T_{c0}(0) \approx 11$ –25 K], all the results confirming the CG scaling law behavior. For simplicity, we present only a detailed description for a nearly optimally doped thin film [linear normal state $R(T)$ curve]. The film (500 nm thick) is patterned in the form of a bridge of rectangular size $100 \mu\text{m}$ wide and $1000 \mu\text{m}$ long with voltage pickup electrodes separated by about $210 \mu\text{m}$ from the center of the bridge. The electrodes, larger than 1 mm^2 each, are made by sputtering silver. Pt wires are bonded by silver epoxy on the electrodes, and the Bi-2201 thin film is baked in a furnace at 350°C in an oxygen atmosphere for 24 h. A Keithley 182 nanovoltmeter and a Keithley 220 current source are used. Pulsed $100 \mu\text{A}$ current is applied for the resistive transition measurements. The temperature stability is better than 0.1 K during the I - V isotherm measurements. Magnetic fields are applied parallel to the c axis (perpendicular to the CuO_2 layers).

Figure 1(a) shows the resistance data, $R(T, H)$ curves, in magnetic fields up to 5.0 T. In Table I, the T_{c0} values in Eq. (2) are given as determined from the linear extrapolation of $\partial T/\partial \ln R(T, H)$ to the T axis ($\partial T/\partial \ln R = 0$) for the linear resistance data ($I \sim V$). Figure 1(b) shows $\alpha(H)$ versus T curves for magnetic fields equal to 0.0, 0.3, 1.0, 2.0, and 3.0 T. We can see that the T_{c0} data (open square symbols) in Fig. 1(b) are very similar to the KT transition temperature determined with $\alpha = 2$. As a result, $T_X(H)$ is the only freely adjustable parameter in the scaling procedure.

Figure 2(a) shows the corresponding CG scaling result for the $R(T, H)$ curves with all the low resistance data being reduced to a universal curve for $1 < X < 16$. Note that the Eq. (3) description (solid line) approach is very good for $1.3 < X < 16$ corresponding to $3.4 \times 10^{-4} < R(T, H)/R_N < 0.32$, where $R_N = R(T = 50 \text{ K}, H = 0)$. Figure 2(b) represents the $\alpha(T, H)$ scaling curve. All $\alpha(T, H) \leq 12$ values collapse onto a single curve [6]. Furthermore, as shown in the inset of Fig. 2(c), for $\alpha T \leq 20$ we find that the temperature dependence of $\alpha(T, H \neq 0)T$

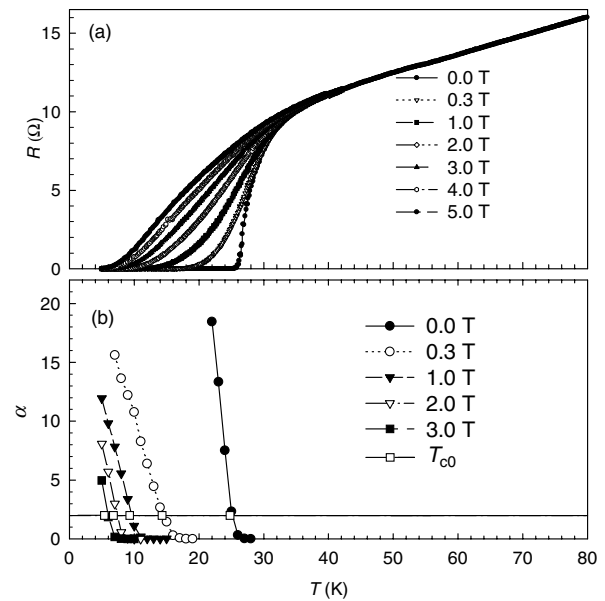


FIG. 1. (a) $R(T, H)$ transition curves in magnetic fields up to 5 T. (b) $\alpha(H)$ as a function of T .

corresponds to another universal scaling. The $\alpha(T, H \neq 0)T$ curves have a common onset point $X_Y \approx 1.2$, corresponding approximately to $T_Y(H)$ s in different magnetic fields. From Fig. 2(c), for the approximately linear part of the scaling curves, we deduce a useful relation of the form $\alpha T \approx f(H)(1 - T/T_Y) \approx f^*(X)(1 - X/X_Y)$, where f is only a magnetic field dependent function for $T < T_Y$, and f^* is a corresponding scaling function for $X < X_Y$.

Figure 3(a) represents $T_{c0}(H)$ together with $T_X(H)$, and $T_i(H)$, where i denotes the resistance ratios $R(T, H)/R_n(T)$, $R_n(T)$ being derived by extrapolation of the normal state resistance at low temperature. The field curves show upward curvatures for small resistance ratios, while they show downward curvatures for large values. We notice that the $T_X(H)$ [except $T_X(H = 0)$] curve is positioned between the $T_{50\%}(H)$ and $T_{60\%}(H)$ curves. By linear extrapolation of the $T_X(H)$ curve to $H = 0$ and $T = 0$, we find the corresponding intercepts: $T_c(H = 0) = 28.2 \pm 0.3 \text{ K}$ and $H_c(T = 0) = 13.7 \pm 0.5 \text{ T}$, respectively, where H_c is the critical magnetic field at zero temperature and $T_c(0)$ is the mean field transition temperature at zero field.

TABLE I. CG scaling and activation energy parameters of the Bi-2201 thin film.

$\mu_0 H$ (T)	T_{c0} (K)	T_X (K)	U_0 (K)	f (K)
0.0	...	27.0	...	1313
0.3	14.3	27.6	252	284
1.0	9.3	26.5	116	179
2.0	6.8	24.6	78.3	124
3.0	5.4	22.3	60.8	92.8
4.0	4.5	20.0	48.9	...
5.0	3.9	18.1	40.7	...

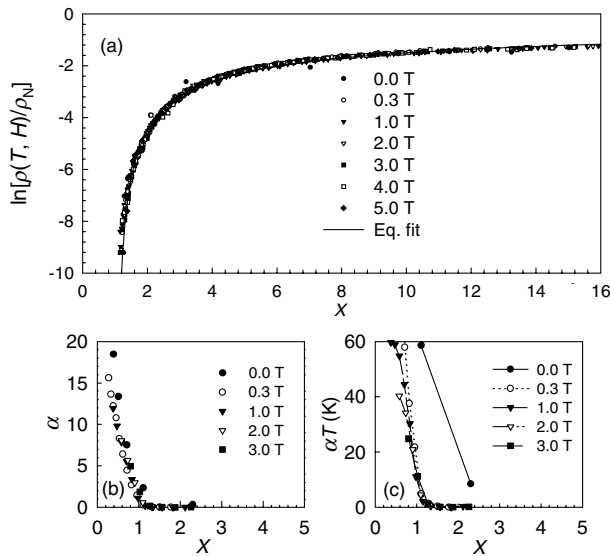


FIG. 2. (a) CG scaling of the resistive transition in different magnetic fields up to 5.0 T. The solid line corresponds to Eq. (3). (b) $\alpha(T, H)$ scaling curve. (c) $\alpha(T, H)T$ scaling curve.

Recently, many studies have suggested that the magnetic phase transition lines are related to a field dependence: $H \sim [1 - T/T_c(0)]^n$ [22–26], where $T \in [T_{c0}(H), T_X(H), T_i(H)]$, and n is a characteristic exponent. In this study, we found $T_c(0) = 28.2$ K. Figure 3(b) shows H as a function of $[1 - T/T_c(0)]$. The variation of the slope gives the n values for the different temperature parameters. The plot gives $n_{c0} = 5.0 \pm 0.3$ and $n_X = 0.98 \pm 0.05$ for $T_{c0}(H)$ and $T_X(H)$, respectively. The n_i value de-

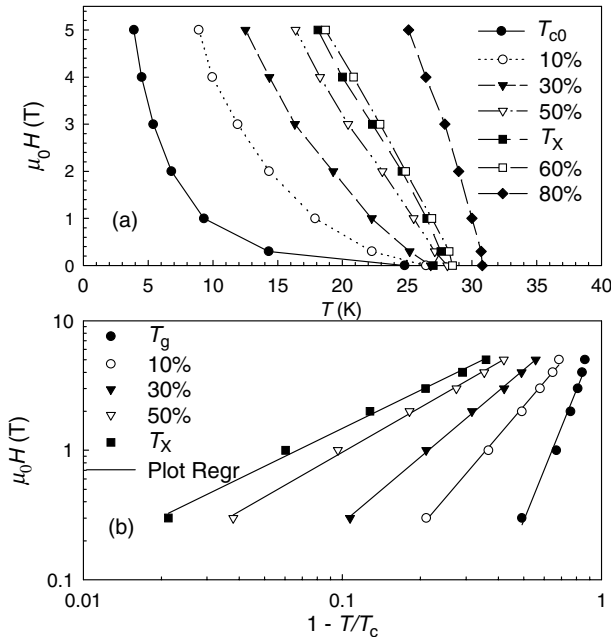


FIG. 3. (a) H - T phase diagram, where $T \in [T_{c0}(H), T_X(H), T_i(H)]$ with i denoting the resistive criteria. (b) H phase diagram as a function of $[1 - T/T_c(0)]$.

creases as i increases. This is a distinct difference from the results obtained for $\text{YBa}_2\text{Cu}_3\text{O}_7$ where n_i is almost constant for $i < 50\%$ [22–26]. The very large exponent for $T_{c0}(H)$ is evidence for the highly quasi-2D effect as already mentioned by other authors [23–26], and in agreement with the analysis of the irreversibility line of a Bi-2201 single crystal reported recently [27].

Figure 4(a) shows a plot of the linear resistance versus $1/T$ in different magnetic fields using a limiting resistive criterion $R/R_N < 10\%$. Assuming Arrhenius type relations:

$$R = R_{\pm} \exp[-U_{\pm}(T, H)/T], \quad (4)$$

we can derive R_{\pm} and U_{\pm} , the resistive prefactors and activation energies for the linear (denoted with “+”) and nonlinear (denoted with “-”) resistances. The activation energy of the resistance can be expressed as $U_+ \approx U_0(H)(1 - T/T_c)$ (for $\alpha \approx 0$) in a linear approach [28], where U_0 is a magnetic field dependent function. Using this relation and Eq. (2), we then obtain

$$U_+/T \approx U_X[T_{c0}(T_c - T_X)/T_c(T_X - T_{c0}) + 1/X], \quad (5)$$

where $U_X = U_0/[(T_X T_{c0})/(T_X - T_{c0})]$.

Figure 4(b) shows the $U_0(H)$ and $T_X T_{c0}/(T_X - T_{c0})$ curves, respectively. We find that $T_X T_{c0}/(T_X - T_{c0}) \propto H^{-0.63}$ which coincides with $U_0(H) \propto H^{-0.63}$. Our CG studies of other Bi-2201 thin films with different $T_{c0}(0)$ s confirm that the relation $U_0(H) \sim T_X T_{c0}/(T_X - T_{c0})$ is

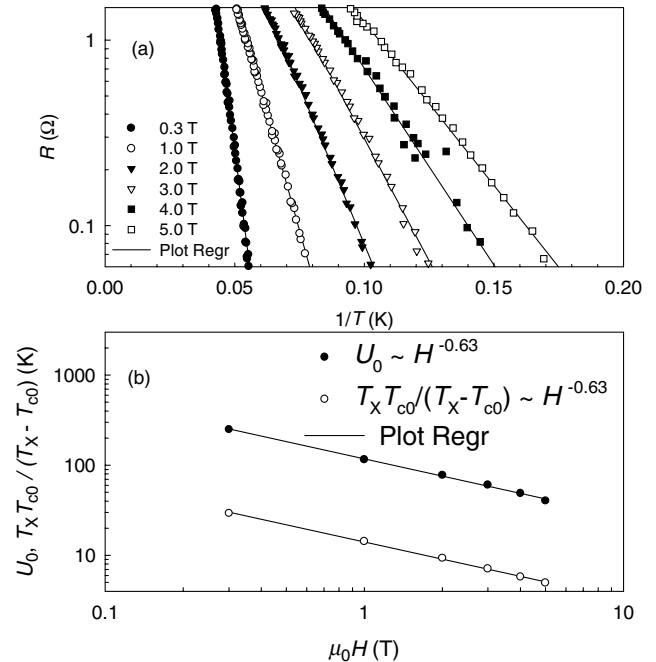


FIG. 4. (a) Arrhenius plot of $R(T, H)$ curves. (b) $U_0(H)$ and $T_n(H)$ in a log-log scale. The solid lines correspond to linear fits.

also obeyed, suggesting that the value of U_X is independent of the magnetic field. From Fig. 2(a), we notice that the CG scaling curve leads for a single Arrhenius function of $1/X$. Assuming $T_c = T_X$, we have $U_+/T \approx U_X/X$ from Eq. (5) resulting in a single function $R \sim \exp(-U_X/X)$ for a simple approach.

With the power law relation, $R = V/I \sim I^\alpha$ ($\alpha > 0$ and $T < T_Y$), we can define the nonlinear resistance as $R = R_-(I/I_0)^\alpha$. Using Eq. (4), we then have

$$U_-/T \approx -\alpha \ln I/I_0, \quad \text{for } \alpha > 0, \quad (6)$$

where I_0 is a constant with $I/I_0 \ll 1$. This relation coincides with the result of Zeldov *et al.* [29] and results in $U_-(T, H) = U_-(X) \approx f^*(X)(1 - X/X_Y) \ln I_0/I$. Note that U_- depends on I , while U_+ does not depend on I for $I \rightarrow 0$; the significance of U_- is that $U_- \rightarrow \infty$ for $I \rightarrow 0$, thus leading to the zero resistance (a true superconducting state). Table I shows the corresponding data derived from these CG scaling analyses.

In summary, a modified CG scaling law is proposed and applied to study the transport properties of Bi-2201 thin films. This CG scaling allows all the magnetic field dependent low resistance data to fall onto a single curve. The temperature dependence of the magnetic phase diagram is obtained and discussed. From this CG scaling and experimental data, a phenomenological relation between the activation energy and the CG scaling parameters is obtained.

We would like to thank Dr. W. Stone, Dr. H. H. Wen, and J. F. de Marneffe for helpful suggestions. This work has been supported by Climb Project of China and PAI 4/10 (Belgium).

[1] G. Blatter, M. Feigel'man, V. Geshkenbein, A. Larkin, and V. Vinokur, *Rev. Mod. Phys.* **66**, 1125 (1994).
 [2] E. H. Brandt, *Rep. Prog. Phys.* **58**, 1465 (1995).
 [3] L. F. Cohen and H. J. Jensen, *Rep. Prog. Phys.* **60**, 1581 (1997).
 [4] J. M. Kosterlitz and D. J. Thouless, *J. Phys. C* **6**, 1181 (1973).
 [5] B. I. Halperin and D. R. Nelson, *J. Low Temp. Phys.* **36**, 599 (1979).
 [6] P. Minnhagen, *Rev. Mod. Phys.* **59**, 1001 (1987); P. Minnhagen and P. Olsson, *Phys. Rev. Lett.* **67**, 1039 (1991); P. Minnhagen, *Phys. Rev. B* **44**, 7546 (1991); P. Minnhagen and P. Olsson, *Phys. Rev. B* **45**, 5722 (1992).
 [7] H. Weber and P. Minnhagen, *Phys. Rev. B* **38**, 8730 (1988); H. Weber, M. Wallin, and H. J. Jensen, *Phys. Rev. B* **53**, 8566 (1996).
 [8] H. J. Jensen and P. Minnhagen, *Phys. Rev. Lett.* **66**, 1630 (1991).

[9] T. G. Holesinger, D. J. Miller, L. S. Chumbley, M. J. Kramer, and K. W. Dennis, *Physica (Amsterdam)* **202C**, 109 (1992).
 [10] D. C. Sinclair, S. Tait, J. T. S. Irvine, and A. R. West, *Physica (Amsterdam)* **205C**, 323 (1993); D. C. Sinclair, J. T. S. Irvine, and A. R. West, *Jpn. J. Appl. Phys. Lett.* **29**, L2002 (1993).
 [11] B. Sales and B. Chakoumakos, *Phys. Rev. B* **43**, 12994 (1991).
 [12] N. R. Khasanova and E. V. Antipov, *Physica (Amsterdam)* **246C**, 241 (1995).
 [13] Y. Murakoshi, S. Kambe, and M. Kawai, *Physica (Amsterdam)* **178C**, 71 (1993).
 [14] S. Martin, A. T. Fiory, R. M. Fleming, L. F. Schneemeyer, and J. V. Waszczak, *Phys. Rev. B* **41**, 846 (1990).
 [15] Y. Z. Zhang, L. Li, D. G. Yang, B. R. Zhao, H. Chen, C. Dong, H. J. Tao, H. T. Yang, S. L. Jia, B. Yin, J. W. Li, and Z. X. Zhao, *Physica (Amsterdam)* **295C**, 75 (1998); Y. Z. Zhang, Y. L. Qin, R. Deltour, H. J. Tao, L. Li, and Z. X. Zhao, *Physica (Amsterdam)* **322C**, 73 (1999).
 [16] T. R. Lemberger, in *Physical Properties of High Temperature Superconductors*, edited by D. M. Ginsberg (World Scientific, New York, 1992), Vol. III, p. 471.
 [17] M. P. A. Fisher, *Phys. Rev. Lett.* **62**, 1415 (1989); D. S. Fisher, M. P. A. Fisher, and D. A. Huse, *Phys. Rev. B* **43**, 130 (1991).
 [18] R. H. Koch, V. Foglietti, W. J. Gallagher, G. Koren, A. Gupta, and M. P. A. Fisher, *Phys. Rev. Lett.* **63**, 1511 (1989).
 [19] H. Yamasaki, K. Endo, S. Kosaka, M. Umeda, S. Yoshida, and K. Kajimura, *Phys. Rev. B* **50**, 12959 (1994).
 [20] P. Wagner, U. Frey, F. Hillmer, and H. Adrian, *Phys. Rev. B* **51**, 1206 (1995).
 [21] M. Andersson, P. Fivat, L. Fàbrega, H. Obara, M. Decroux, J.-M. Triscone, and Ø. Fischer, *Phys. Rev. B* **54**, 675 (1996).
 [22] M. Tinkham, *Phys. Rev. Lett.* **61**, 1658 (1988).
 [23] C. C. Almasan, M. C. de Andrade, Y. Dalichaouch, J. J. Neumeier, C. L. Seaman, M. B. Maple, R. P. Guertin, M. V. Kuric, and J. C. Garland, *Phys. Rev. Lett.* **69**, 3812 (1992).
 [24] A. Schilling, R. Jin, J. D. Guo, and H. Ott, *Phys. Rev. Lett.* **71**, 1899 (1993).
 [25] J. Deak, L. Hou, P. Metcalf, and M. McElfresh, *Phys. Rev. B* **51**, 705 (1995).
 [26] L. Hou, J. Deak, P. Metcalf, M. McElfresh, and G. Preosti, *Phys. Rev. B* **55**, 11806 (1997).
 [27] A. Morello, A. G. M. Jansen, R. S. Gonnelli, and S. I. Vedenev, *Phys. Rev. B* **61**, 9113 (2000).
 [28] T. T. M. Palstra, B. Batlogg, R. B. van Dover, I. F. Schneemeyer, and J. V. Waszczak, *Phys. Rev. B* **41**, 6621 (1990).
 [29] E. Zeldov, N. M. Amer, G. Koren, A. Gupta, R. J. Gambino, and M. W. McElfresh, *Phys. Rev. Lett.* **62**, 3093 (1989); E. Zeldov, N. M. Amer, G. Koren, A. Gupta, M. W. McElfresh, and R. J. Gambino, *Appl. Phys. Lett.* **56**, 680 (1990).